THE BAROCLINIC FORCING OF THE SHEAR LAYER THREE-DIMENSIONAL INSTABILITY

Laurent Joly, Jean Reinaud*
Department of Fluid Mechanics, ENSICA
1, Pl. E. Blouin, 31056 Toulouse, France
laurent@ensica.fr, jean@mcs.st-and.ac.uk

Patrick Chassaing
Institut de Mécanique des Fluides de Toulouse
Allée du Prof. C. Soula, 31400 Toulouse, France
chassain@ensica.fr

ABSTRACT

Some new elements about the transition to three-dimensionality of variable density mixing layers are proposed. The two-dimensional action of the baroclinic torque is examined from the strain fields. It is seen to yield drastically enhanced strain rates in the core region. Then the consequence on the development of three-dimensional instabilities is detailed and the asymmetric development of the streamwise ribs is described. The streamwise circulation is shown to be preferentially generated on the heavy-side of the core and the mechanism of the translative instability is surprinsingly preserved. Compared to the constant density situation, the amplification of the 3D modes is lower and their onset is slightly delayed.

INTRODUCTION

The generation-destruction of vorticity by the baroclinic torque may substantially alter the transition dynamics of shear flows. In the two-dimensional stratified mixing layer under the Boussinesq approximation, Staquet (1995) described small-scale secondary eddies located at the saddle points between large-scale structures on so-called baroclinic layers. The three-dimensional study of such a situation lead Showalter *et al.* (1994) to stress that baroclinically generated, or enhanced, vortices may possibly result in an earlier transition to turbulence. In compressible mixing layers, Lele (1989) or Sarkar & Pantano (2000) stressed the consequences of high density ratios.

The present contribution deals with the baroclinic effects beyond the Boussinesq approximation but uncorrelated to compressibility. The baroclinic torque results from the inertial component of the pressure gradient only. The vorticity evolves within a quasi-solenoidal velocity field without suffering from strong dilatational effects that are scaled by any relevant Mach number. This purely inertial influence of density variations is likely to occur in high Reynolds number mixing of fluids of different densities or in thermal mixing. Such variable-density shear-layers were previously considered by Davey & Roshko (1971) who concluded that the situation where the lighter fluid is the faster leads to an increase in the amplification rate of instability oscillations. More recently a step further was achieved in the numerical analysis of Soteriou & Ghoniem (1995) on spatially evolving 2D shear layers. They confirmed that an asymmetric entrainment resulting from the baroclinic torque is responsible for the shifting of the center of the main structures into the lighter fluid, a different convection velocity and a modified spreading rate.

In the variable-density mixing layer the vorticity is redistributed in favor of the light-side vorticity braid, the other being vorticity depleted in a first stage and then fed with a vorticity source of sign opposite to the one of the initial layer, see Reinaud *et al.* (1999). These two opposite-sign vorticity sheets lay around the vanishing primary structure core, still figuring the center of this two-layers system. Then the braids are continuously streched while enrolling towards this center in a spiral like scheme. At infinite Reynolds numbers Reinaud, Joly & Chassaing (2000) showed that the baroclinically enhanced

*the present address of the second author is "School of Mathematics and Statistics, University of St Andrews, St Andrews KY16 9SS, Scotland"

2D vorticity braid is likely to break-up into secondary rollups.

In three-dimensional flows the vorticity dynamics is also affected by the vortex stretching mechanism that enables enstrophy to travel among vorticity components through 3D instability modes. The consequences of the baroclinic redistribution of spanwise vorticity on the development of three-dimensionnal modes is the focus point of the present paper. The interference with the pairing process and further subharmonics emergence is not yet considered.

The experimental evidence, e.g. Bernal & Roshko (1986), the stability analysis of Pierrehumbert & Widnall (1982) and Corcos et Lin (1984), and the direct simulations, e.g. Rogers & Moser (1992), all converge toward a similar route to three-dimensionality leading to streamwise vortices lying in the braid region as a result of both an instability located in the Kelvin-Helmoltz (KH) billow called translative instability (TI) and one located in the vorticity-depleted braid hereafter called shear instability (SI). Knio & Ghoniem (1992) contributed to the first analysis of these co-working mechanisms under non-symmetric vorticity conditions resulting from a weak baroclinic torque. They focussed on symmetry losses and acknowledged for uneven intensification and weakening of the streamwise vorticity.

As stated by these authors the baroclinic torque is responsible for such a different two-dimensional structure that the results on the spanwise stability of Stuart vortices or even the KH billow are irrelevant to the 3D stability properties of the variable-density situation. Though this case demands a currently unavailable stability study, a step further has been attempted in intensifying the density variation and refining the crosswise description of the layer in order to get a full baroclinic torque effect, i.e. opposite-sign vorticity sheets as in Reinaud *et al.* (1999). The core being vorticity depleted in favor of surrounding vorticity cups, the translative instability mechanism is expected to weaken leaving vorticity cups submitted to the braid instability. This scenario is examined in the last part of the paper.

PRELIMINARIES

The baroclinic torque

The baroclinic effect is the additional torque that is felt when an inhomogeneous mass field is submitted to a pressure gradient normal to the local density gradient. In the limit of inviscid two-dimensional incompressible flows, the baroclinic torque is the only source of vorticity variation along the particle path, as stated by the corresponding vorticity equation :

$$\mathrm{d}_t\,\omega = -\frac{1}{\rho^2}\boldsymbol{\nabla}P \times \boldsymbol{\nabla}\rho \qquad (1)$$

where $\mathrm{d}_t = \partial_t + \mathbf{u}\cdot\boldsymbol{\nabla}$ is the material derivative. In this simplified situation the pressure gradient is directly connected to the material acceleration $\mathbf{a} = \mathrm{d}\mathbf{u}/\mathrm{d}t$ such that the baroclinic torque $\mathbf{b}$ is given by :

$$\mathbf{b} = \mathbf{a} \times \boldsymbol{\nabla}(\ln\rho) \qquad (2)$$

Hence the interpretation of the baroclinic torque as being of inertial nature. This simple scheme is the one that acts primarily on the spanwise rollers of the KH instability leading firstly to a strong asymmetry of the vorticity field, and further on yielding the concentration of the circulation on thinning vorticity sheets of opposite signs, see figure 1. In three-dimensions the vorticity budget is complemented with the vortex stretching term and in real flows viscosity acts at the diffusion of vorticity gradients. At the zero Mach number limit, dilatation results from density diffusion only. The divergence of the velocity field being $s = \boldsymbol{\nabla}\cdot\mathbf{u}$ and ϱ standing for $(\ln\rho)$, the continuity equation turns into an advection-diffusion equation :

$$\mathrm{d}_t\varrho = \mathcal{D}\Delta\varrho = -s \qquad (3)$$

Provided $\pi = p/\rho + u^2/2$ is the specific pressure head, the momentum equation can be recasted in the following form :

$$\partial_t\mathbf{u} = \mathbf{u}\times\boldsymbol{\omega} - \boldsymbol{\nabla}\pi - \frac{p}{\rho}\boldsymbol{\nabla}\varrho + \nu\Delta\mathbf{u} \qquad (4)$$

The numerical procedure

These equations are solved for the temporal mixing layer with the streamwise (x) velocity profile in the crosswise (z) direction :

$$u_x = U\mathrm{erf}(\pi^{1/2}\frac{z}{\delta_\omega^0}) \qquad (5)$$

Streamwise and spanwise (y) periodic conditions are imposed within a classical pseudo-spectral approach on a mesh counting up to 192×96×264 nodes yielding Reynolds numbers, based on the initial vorticity thickness, of 500. The density ratio of the upper to the lower streams has been set to 3. Harmonic perturbations of equal intensities are imposed

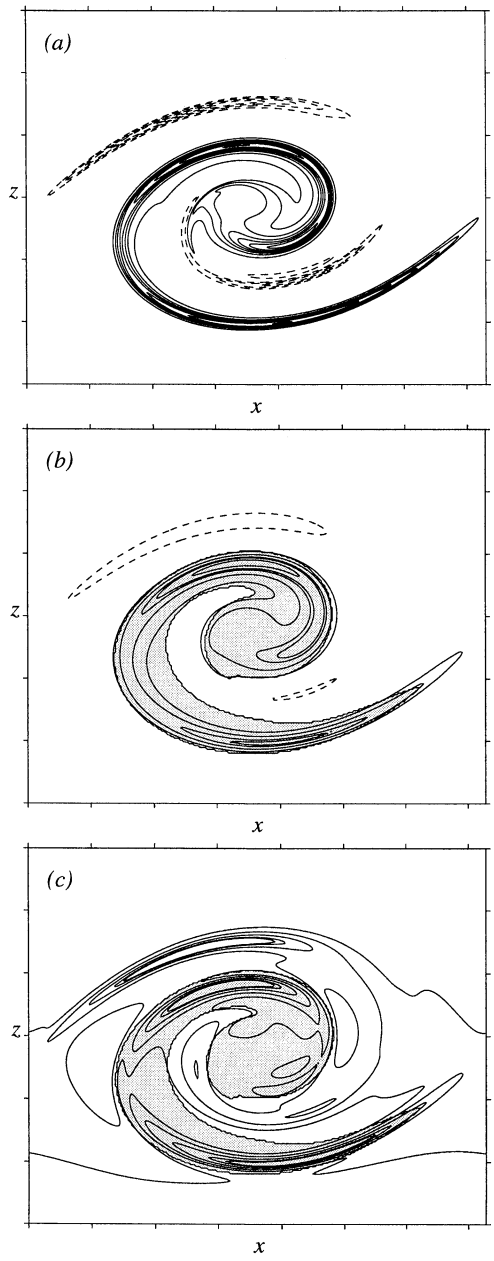

Figure 1: Spanwise vorticity ω_y contours of the two-dimensional variable density mixing-layer at $t = 12$: (a) $\mathcal{R}_e = U\delta^0_\omega/\nu = 3000$ (b) $\mathcal{R}_e = 500$. The density ratio $S_\rho = \rho_{\text{upper}}/\rho_{\text{lower}} = 3$. (c) contours of the strain ϵ in the sense of Caulfield and Kerswell (2000) : contour increment is $U/3\delta^0_\omega$. Shaded region where rotation prevails over strain according to CK.

to promote the KH and the spanwise instabilities. The two-dimensional mode is perturbated with the eigenfunctions of the most unstable mode $\alpha_{2D} = 2\pi/\lambda_x = 0.48\sqrt{\pi}/\delta^0_\omega$ given by the constant density linear stability analysis. In the variable density case, a global convection velocity, $-u_c$, opposite to the group velocity of the 2D perturbation, is added to the velocity profile (5) in order to keep the main structure centered in the temporally evolving frame. The three-dimensional mode is choosen

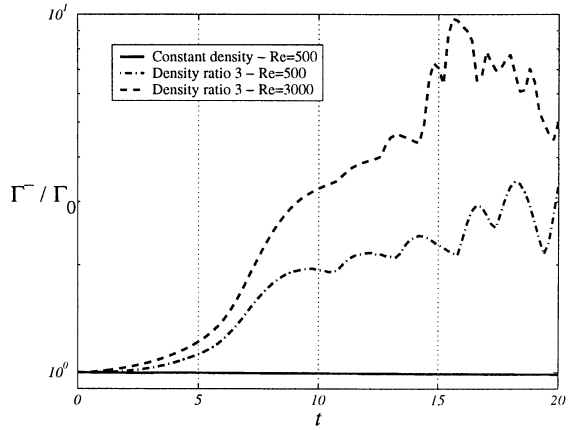

Figure 2: The increase of the circulation Γ^- associated with baroclinically enhanced negative regions of vorticity, non-dimensioned by the initial circulation $\Gamma_0 = -2\lambda U$.

as $\lambda_y = 0.5\lambda_x$, close to the most unstable wavelength given by the stability analysis of Stuart vortices by Pierrehumber & Widnall (1982). Its shape is the streamwise invariant rod (STI) used in the three-dimensional stability analysis of Rogers & Mosers (1992). As in Knio & Ghoniem (1992), the characteristic scales and initial conditions are the same between the constant and variable density simulations.

THE STRAIN RATE OF THE 2D MIXING LAYER

Since the baroclinic torque is strongly dependent on the density gradients it is also sensitive to the Reynolds number. Figures 1(a) and (b) illustrate the structure of the two-dimensional vorticity field of mixing-layers with density ratio of 3 and Reynolds numbers (based on the initial vorticity thickness) of 500 and 3000, respectively.

Though the growth of the primary mode energy is only weakly affected by the baroclinic torque (not shown), it is striking how the amounts of negative and positive circulation associated with that vorticity source is anything but negligeable against the initial circulation in the period. It is straightforward to show that the latter is $\Gamma_0 = -2U\lambda$ where λ is the period length. Figure 2 illustrates the departure of the negative circulation Γ^- from that value. Since the circulation is an invariant of the problem, a corresponding positive circulation is generated on heavy-side braids, see Reinaud *et al.* 2000. Again, the higher the Reynolds number the more significative is the departure from the constant density situation.

As far as the three-dimensionalization of this flow is concerned, a description of the

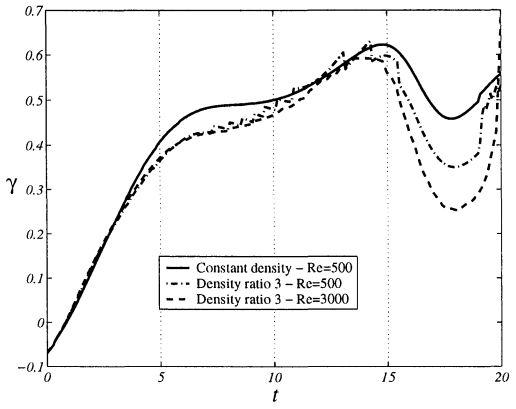

Figure 3: The evolution of the strain γ normal to the density gradient at the saddle point between the main 2D structures.

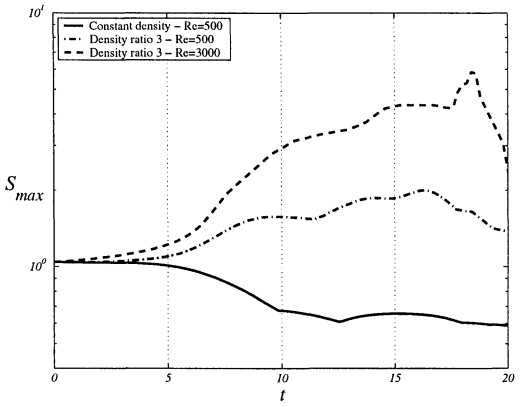

Figure 4: The evolution of the maximum strain rate S_{max} (positive eigenvalue of tensor $\mathcal{D}$) over the entire domain.

2D strain field is needed. The strain tensor $\mathcal{D} = (\nabla \mathbf{u} + \nabla \mathbf{u}^t)/2$ is projected there in the direction of the unitary vector $\mathbf{n}$ normal to the local density gradient conformly to, e.g. Ottino (1989), : $\gamma = \mathcal{D} : \mathbf{nn}$. Figure 3 shows how the evolution of the stain rate at the saddle point region is weakly affected by the redistribution of vorticity in the main structure.This results from the conservation of the overall circulation within the period, see Corcos & Sherman (1984). But this global invariance statement does not extend to local amounts of spanwise circulation. From figure 1(c) it is clear that the strain field looses the symetry of the constant density roll-up. Compared to the contours of ϵ together with the rotation-dominated shaded region by Caulfield & Kerswell (2000), it turns out that the upper braid (heavy fluid side) is the region of maximum strain rate and minimum rotation. Figure 4 confirms that much higher levels of strain are produced there under the action of the baroclinic torque. This is retained as a main difference expected to affect the development of streamwise structures

Name	ρ_{up}/ρ_ℓ	$\mathcal{R}_e$	N_x	u_c	Γ_x/Γ_y^0
PS	/	500	128	0.	0.023
VD	3	500	192	0.28	0.023

Table 1: .Global parameters of the passive scalar and baroclinically modified three-dimensional simulations

in 3D mixing layers through the SI mechanism.

THE STRUCTURE OF THE 3D SHEAR-LAYER

Two simulations are analysed in this paper, one solving the passive scalar (PS) equations and the other (VD) with full variable density effects. The parameters of the PS and VD cases are reported in table 1. Throughout the paper, time is normalized by $\tau = \delta_\omega^0/U$, vorticity by the initial maximum $2U/\delta_\omega^0$ and strain by $1/\tau$. Unless quoted, the vorticity contours increment is always U/δ_ω^0 starting from zero. The positive vorticity contours are sketched by solid lines and negative contours by dashed ones. The tic marks along the spatial coordinates are distributed every δ_ω^0.

The spanwise vorticity

The structure of the spanwise vorticity cross-section is derived directly from the folded distribution established in 2D. In both the rib plane and the "off-rib" one, spanwise vorticity is redistributed in thin sheets of alternate signs. The contour maps given in figure 5, taken at $t = 8$, are still simple. In the "off-rib" base plane, cutting the center of the upper spanwise mushroom structure, two counter-rotative thin vorticity layers are brought closer to each other than in the 2D case, locally defining a jet flow of light fluid towards the heavy side. In the rib plane, the sketch is quite similar, though no more symetric, to the one given by Rogers & Mosers (1992) fig. 19(a). The analysis of subsequent spanwise vorticity maps is more difficult due to the complex structure of the core region as seen from the streamwise vorticity contours of figure 8.

The rib vortices

Streamwise vorticity is collapsing into rib vortices as in the constant density case. At $t = 8$, figure 6 indicates that the streamwise structure is growing more rapidly on its right side lying above the main structure. This can be clearly associated with the favourable effect of the additional strain in that region, as mentioned in the 2D analysis. A weak region of negative streamwise vorticity is also noted at the center of the core and is the signature

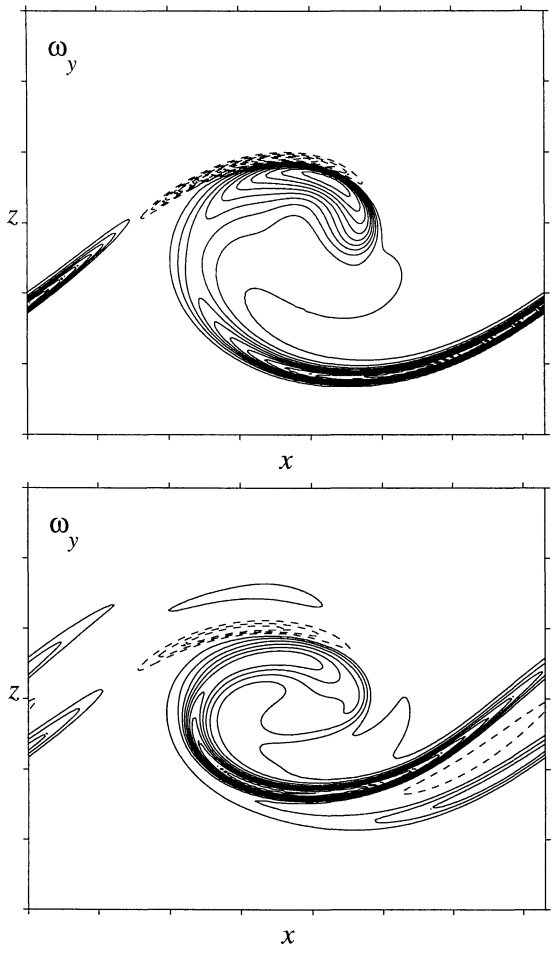

Figure 5: Contours of spanwise vorticity ω_y of the three-dimensional variable density mixing-layer at $t = 8$. Top : Base Plane cross section, bottom: Rib Plane cross section.

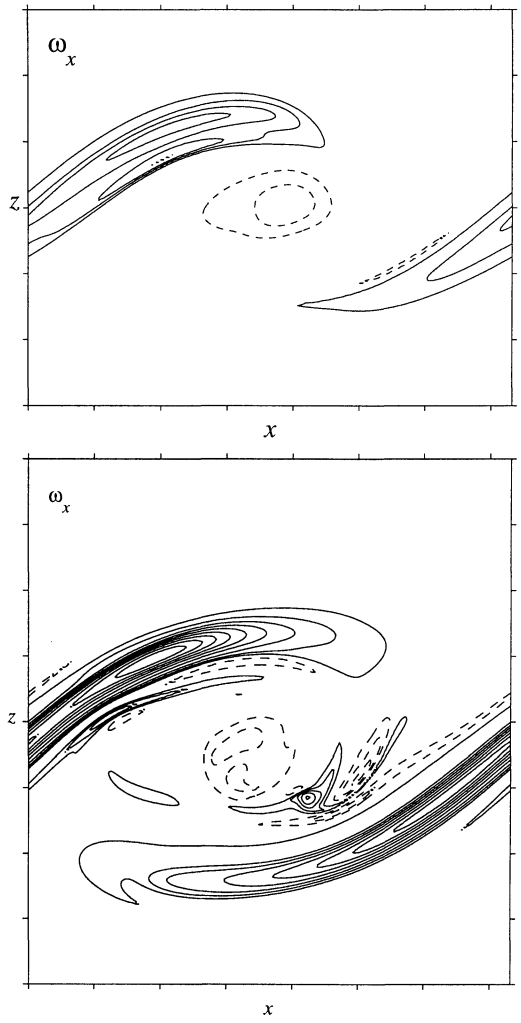

Figure 6: Contours streamwise vorticity ω_x at $t = 8$ (top) and $t = 12$ (bottom). Contour increments is U/δ^0_ω, tic marks are at δ^0_ω.

of the still active translative instability mechanism. At $t = 12$ the main contribution to the streamwise circulation comes from the dominant rib vortices, see figure 7. The mechanism acting on spanwise vorticity in 2D, namely the baroclinic source on the light side and sink on the heavy side, is recovered in the streamwise direction. From figure 8 (right views) the rib vortices are developing with a companion counter-rotative layer on the heavy side. This association yields again a higher entrainment of light fluid into the heavy medium as seen from the density half maps.

Analysis of the growth of 3D modes

The spatial structure of the rib vortices is seen to be affected by the modified strain field and by the streamwise baroclinic torque. The sensitivity of the amplification rate of the three-dimensional modes to these changes is discussed. Figure 9 gives the time evolution of the energy content of the pure two-dimensional mode A_{10}, corresponding to the streamwise and spanwise wavenumbers $(k_x, k_y) = (2\pi/\lambda_x, 0)$, and of the cumulated three-dimensional modes , i.e. those which satisfy $k_y \neq 0$. In this semilog plots the slopes of linear portions are equivalent to the exponential amplification rates of the small perturbations. Both the PS and VD cases undergo a two-stage evolution for A_{3D} , the first one connected with the growing 2D mode and the second one specific of the three-dimentionalization of the flow. The VD exhibits a delayed transition at $t = 12$ (9 for PS) and a lower amplification rate $\sigma_{3D-VD} = \sigma_{3D-PS}/2$. This first conclusion stands for the linear response of the layer to the presently small perturbations. The non-linear regime as well as the higher Reynolds number domains have to be further explored.

REFERENCES

Bernal, L.P. and Roshko, A., 1986, *J. Fluid*

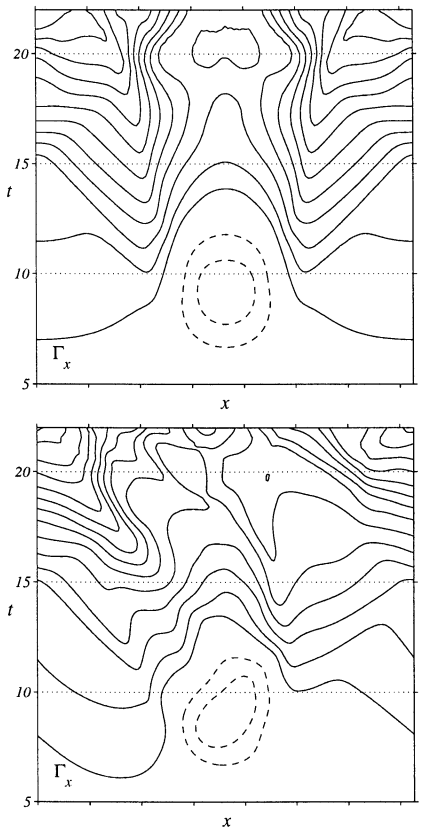

Figure 7: Time evolution of the streamwise circulation $\Gamma_x(x,t)$. Top : passive scalar, bottom : variable density.

Mech., vol. 170, pp. 499.

Corcos, G.M., and Sherman. F.S., 1984, *J. Fluid Mech.*, vol. 139, pp. 29.

Caulfield, C.P. and Kerswell, R.R., 2000, *Phys. Fluids*, vol. 12(5), pp. 1032.

Knio, O.M. and Ghoniem, A.F., 1992, *J. Fluid Mech.*, vol. 243, pp. 353.

Lele, S., 1989, *CTR Report N89-22827.*

Ottino, J.M., 1989 *The kinematics of mixing: stretching, chaos and transport*, CUP.

Pierrehumbert, R.T. and Widnall, S.E., 1982, *J. Fluid Mech.*, vol. 114, pp. 59.

Reinaud, J., Joly, L. and Chassaing, P., 1999, *TSFP-1*, Santa-Barbara.

Reinaud, J., Joly, L. and Chassaing, P., 2000, *Phys. Fluids*, vol. 12, pp 2489.

Rogers, M.M. and Moser, R.D., 1992, *J. Fluid Mech.*, vol. 243, pp. 183.

Sarkar, S. and Pantano, C., 2000, *Int. Conf. on Variable Density Turbulent Flows*, France.

Schowalter, D.G., Van Atta, C.W. and Lasheras, J.C., 1994, *J. Fluid Mech.*, vol. 281, pp. 247.

Soteriou, M.C. and Ghoniem, A.F., 1995, *Phys. Fluids A*, vol. 7(8), pp. 2036.

Staquet, C., 1995, *J. Fluid Mech.*, vol. 296, pp. 73.

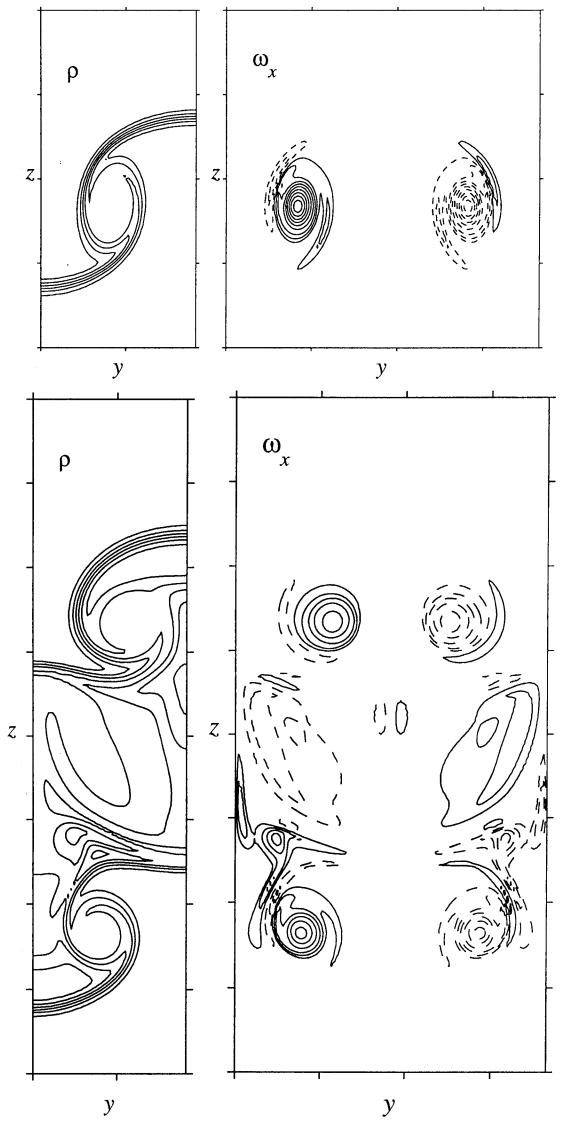

Figure 8: Contours of density and streamwise vorticity of the three-dimensional variable density mixing-layer at $t = 12$. Contour increments for the density (left) are $\Delta\rho/6$. Top : Mid-braid cross section, bottom: Core plane cross section.

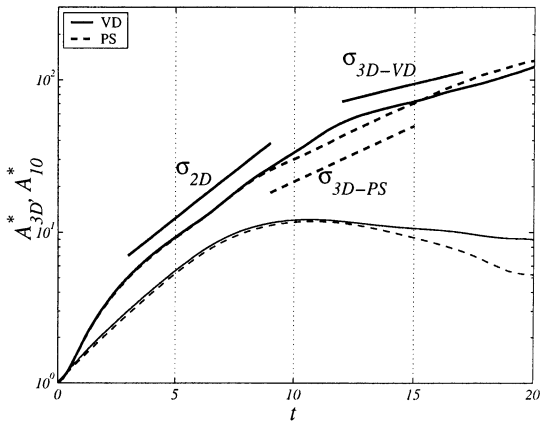

Figure 9: Time evolution of the normalized energy in all three-dimensional modes A_{3D} and in the two-dimensional one A_{10}.